care alone. Therefore, there is an emergent need for effective second-line treatments for NSCLC patients who experience disease progression after first-line chemotherapy. Currently, erlotinib, docetaxel, and pemetrexed are approved as second-line drugs by the US Food and Drug Administration for patients whose tumors have progressed after platinum-based treatments [4, 5].

Small cell lung cancer (SCLC) accounts for approximately 12% of all lung cancers [6]. Compared with NCSLC, SCLC has a rapid doubling time, and earlier development of wide spread metastasis. SCLC is highly sensitive to initial radiotherapy and chemotherapy. The most commonly used regimens include etoposide, cisplatin, doxorubicin, or cyclophosphamide [7]. For limited-stage patients, chemotherapy associated with thoracic radiation was able to produce a cure rate of 10–20%. In extensive disease, the combinations of these agents yields responses of 50–70%, with 20–30% complete remissions, but most patients die from recurrent diseases. The identification of new agents is critical for further progress in the treatment of SCLC, and the evaluation of a variety of agents including docetaxel and pemetrexed has been underway [8–10].

Pemetrexed is a new antifolate that has significant activity against a broad spectrum of solid tumors including lung cancer [11, 12]. Pemetrexed inhibits multiple enzymes involved in folate metabolism including thymidylate synthase, dihydrofolate reductase, and glycinamide ribonucleotide formyltransferase [13]. Pemetrexed arrests cells mainly in S phase and induces apoptosis against tumor cells [14]. Against lung cancers, pemetrexed is non-inferior to docetaxel, with lower hematologic toxicity, and febrile neutropenia and a similar rate of non-hematologic toxicities [12].

The taxanes, paclitaxel and docetaxel, have significant activity in lung cancer. Both inhibit microtubule dynamics and cause G2/M cell cycle arrest. However, there are several differences between them in the pharmacokinetics and pharmacologic actions [15, 16]. Docetaxel demonstrated greater affinity for the tubulin-binding site, wider cell cycle activity, longer intracellular retention time and higher intracellular concentration in tumor cells, more potent antitumor activity in in vitro and in vivo models, and more potent induction of bcl-2 phosphorylation and apoptosis. Paclitaxel has a non-linear pharmacokinetic behavior, while docetaxel demonstrated linear pharmacokinetics and less schedule dependence than paclitaxel.

The combination of pemetrexed and docetaxel may play a major role in the second-line treatment of lung cancers. The wide range of antitumor activity of these agents, their different cytotoxic mechanisms and different toxicity profiles, and the absence of cross-resistance provide the rationale for combining these agents. Since both pemetrexed and docetaxel are cell cycle-specific, disturbances of the cell cycle produced by one drug may influence the cytotoxic

effects of the other. Furthermore the drug schedule may play a significant role in the outcome, and therefore, how the drugs are combined requires careful consideration.

We showed that the ordered treatment of pemetrexed followed by paclitaxel may be synergistic, whereas simultaneous administration was potentially antagonistic in a variety of solid tumor cell lines [17]. What is not clear is whether such schedule dependency will be as important for pemetrexed and docetaxel as for pemetrexed and paclitaxel in the treatment of lung cancers. The present study was aimed at characterizing the cytotoxic effects of various pemetrexed and docetaxel combinations and schedules on three human lung cancer cell lines using the isobologram method of Steel and Peckham [18]. Flow cytometry was performed to understand the molecular basis of the schedule-dependent synergism and antagonism of the pemetrexed and docetaxel combination.

Materials and methods

Cell lines

Three human lung cancer lines, A-549 (lung adenocarcinoma), Lu-99 (giant-cell lung cancer), and SBC-5 (small cell lung cancer) were used. A-549 cells were purchased from the American Type Culture Collection (Rockville, MD). Lu-99 and SBC-5 cells were obtained from Health Science Research Resources Bank (Tokyo). These cells were growing as a monolayer in 75-cm^2 plastic tissue culture flasks containing RPMI1640 medium (Sigma Chemical Co., St Louis, MO) supplemented with 10% heat-inactivated fetal bovine serum (FBS) (Sigma) and antibiotics (penicillin G and streptomycin) in a humidified atmosphere of 95% air/5% CO_2 at 37°C. Under these conditions, the doubling times of these cells were 20–30 h.

Drugs

Pemetrexed and docetaxel were kindly provided by Eli Lilly and Company (Indianapolis, IN) and Sanofi-Aventis K.K. (Tokyo, Japan), respectively. Drugs were dissolved with RPMI1640 and stored at −80°C. Drugs were diluted with RPMI-1640 plus 10% FBS before use.

Cell growth inhibition using combined anti-cancer agents

Growing cells were collected by trypsinization, separated and resuspended to a final concentration of 5.0 × 10^3 cells/ml in fresh medium containing 10% FBS and antibiotics. Cell suspensions (100 μl) were dispensed into the individual wells of a 96-well tissue culture plate with a lid (Costar, Corning, NY). Each plate had one 8-well control column

containing medium alone and one 8-well control column containing cells but no drug. Eight plates were prepared for each drug combination.

Simultaneous and continuous exposure to pemetrexed and docetaxel

After a 20–24 h incubation for cell attachment, solutions of docetaxel and pemetrexed (50 µl) at different concentrations were added to individual wells in final volumes of 200 µl per wells. The plates were incubated under the same conditions for 120 h.

Simultaneous 24 h exposure to pemetrexed and docetaxel

After cell attachment, solutions of docetaxel and pemetrexed (50 µl) at different concentrations were added to individual wells in final volumes of 200 µl per wells. The plates were also incubated under the same conditions for 24 h. The cells were then washed twice with culture medium, and then fresh medium (200 µl) and antibiotics were added. The cells were cultured again for four additional days in drug-free medium.

Sequential exposure to pemetrexed (24 h) followed by docetaxel (24 h) or vice versa

After cell attachment, medium containing 10% FBS (50 µl) and solutions of docetaxel or pemetrexed (50 µl) at different concentrations were added to individual wells. The plates were then incubated under the same conditions for 24 h. The cells were washed twice and fresh medium was added, followed by the addition of solutions of docetaxel or pemetrexed (50 µl) at different concentrations. The plates were incubated again under the same conditions for 24 h. The cells were then washed twice, and the cells were cultured for three additional days in drug-free medium.

MTT assay

Viable cell growth was determined by 3-(4,5-dimethylthia-zol-2-yl)-2,5-diphenyltetrazolium bromide (MTT) assay [19]. For all 4 cell lines examined, we established a linear relation between the MTT assay value and the cell number within the range shown.

Isobologram

The dose–response interactions between pemetrexed and docetaxel were evaluated at the IC_{50} level by the isobologram method of Steel and Peckham (Fig. 1) [18]. The IC_{50} was defined as the concentration of drug that produced 50% cell growth inhibition; i.e. a 50% reduction of absorbance.

The theoretical basis of the isobologram method and the procedure for making the isobologram has been described in detail [18, 20, 21]. Based on the dose–response curves of pemetrexed and docetaxel, three isoeffect curves were constructed (Fig. 1). If the agents act additively by independent mechanisms, combined data points would lie near the Mode I line (hetero-addition). If the agents act additively by similar mechanisms, the combined data points would lie near the Mode II lines (iso-addition) [14, 16, 17].

Since we cannot know in advance whether the combined effects of two agents will be hetero-additive, iso-additive, or an effective intermediate between these extremes, all possibilities should be considered. Thus, when the data points of the drug combination fell within the area surrounded by mode I and/or mode II lines (i.e. within the envelope of additivity), the combination was described as additive.

We used this envelope to evaluate not only the simultaneous exposure combinations of pemetrexed and docetaxel, but also to evaluate the sequential exposure combinations, since the second agent under our experimental conditions could modulate the cytotoxicity of the first agent.

A combination that gives data points to the left of the envelope of additivity (i.e. the combined effect is caused by lower doses of the two agents than is predicted) can confidently be described as supra-additive (synergism). A combination that gives data points to the right of the
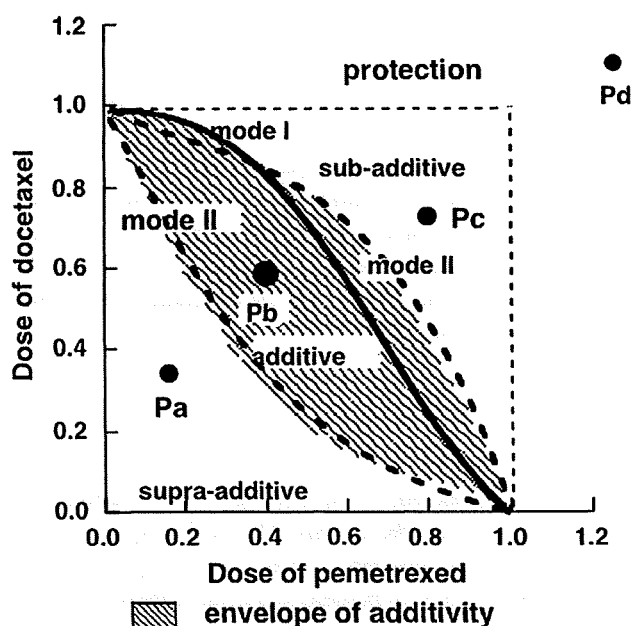

Fig. 1 Schematic representation of an isobologram (Steel and Peckham). The envelope of additivity, surrounded by mode I (solid line) and mode II (dotted lines) isobologram lines, was constructed from the dose–response curves of pemetrexed alone and docetaxel alone. The concentrations that produced 50% cell growth inhibition were expressed as 1.0 in the ordinate and the abscissa. Combined data points Pa, Pb, Pc and Pd show supra-additive, additive, sub-additive, and protective effects, respectively

envelope of additivity, but within the square or on the line of the square can be described as sub-additive (i.e. the combination is superior or equal to a single agent but is less than additive). A combination that gives data points outside the square can be described as protective (i.e. the combination is inferior in cytotoxic action to a single agent). A combination with both sub-additive and/or protective interactions can confidently be described as antagonistic.

Data analysis

Findings were analyzed as described previously [22]. To determine whether the condition of synergism (or antagonism) truly existed, a Wilcoxon signed-rank test was performed to compare the observed data with the predicted minimum (or maximum) data for an additive effect. Probability values $(P) \leq 0.05$ were considered significant. Combinations with $P > 0.05$ were regarded as having an additive/synergistic (or additive/antagonistic) effect. All statistical analyses were performed using the Stat View 4.01 software program (Abacus Concepts, Berkeley, CA).

Flow cytometric analysis

SBC-5 cells were treated with 5.0 μM pemetrexed alone, or 1.5 nM docetaxel alone or their combination simultaneously for 24 h. The cells were also treated with pemetrexed for 24 h followed by docetaxel for 24 h or the reverse sequence. The cells were harvested at 72 h and the cell cycle profiles were analyzed by staining intracellular DNA with propidium iodide in preparation for flow cytometry with the FACScan · CellFIT system (Becton-Dickinson, San Jose, CA). The size of the sub-G1, G0/G1 and S+G2/M fractions was calculated as a percentage by analyzing DNA histograms with the ModFitLT 2.0 program (Verity Software, Topsham, ME) [23].

Results

Figure 2 shows the dose–response curves for pemetrexed in A-549, Lu-99, and SBC-5 cells. The dose–response curves were plotted on a semi-log scale as a percentage of the control. The IC_{50} values of pemetrexed against these cells were 1.5 ± 0.4, 0.42 ± 0.10, 1.3 ± 0.2 μM, respectively $(n = 5)$. The IC_{50} values of docetaxel against these cells were 1.7 ± 0.2, 1.0 ± 0.1, and 0.82 ± 0.13 nM, respectively $(n = 5)$.

The dose–response curves in Fig. 3 show the effect of simultaneous exposure (24 h) (panel a), sequential exposure to pemetrexed followed by docetaxel (panel b), and vice versa (panel c) on the growth of SBC-5 cells. The

Dose-response curves of pemetrexed against lung cancer cell lines
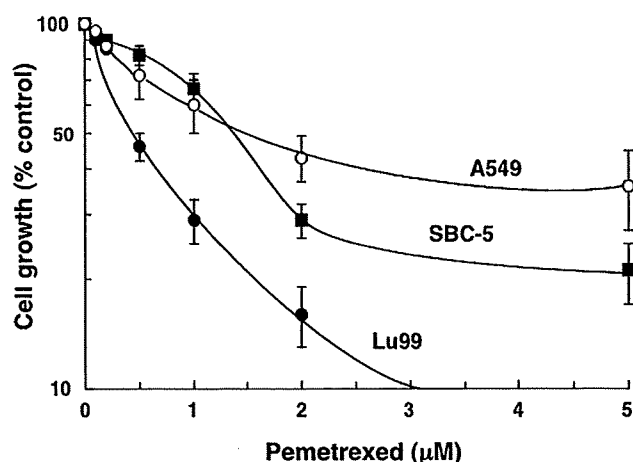

Fig. 2 The dose–response curves of 24 h exposure to pemetrexed against A-549, Lu-99, and SBC-5 cells. Cell growth inhibition was measured using the MTT assay after 5 days and was plotted as a percentage of the control (cells not exposed to drugs). Each point represents the mean ± SEM for at least three independent experiments

pemetrexed concentrations are shown on the abscissa. Dose–response curves in which the docetaxel concentrations are shown on the abscissa are based on the same data (figure not shown). Three isoeffect curves (mode I and mode II lines) were constructed based on the dose–response curves of pemetrexed alone and docetaxel alone. Isobolograms at the IC_{50} level were generated based on these dose–response curves for the combinations.

Simultaneous exposure to docetaxel and pemetrexed for 24 h

Figure 4a shows isobolograms of SBC-5 cells after simultaneous exposure to pemetrexed and docetaxel. The combined data points fell in the areas of subadditivity and protection. The mean values of the observed data (0.71) were larger than those of the predicted maximum values (0.60). The observed data and the predicted maximum data were compared by Wilcoxon signed-rank test. The difference was significant $(P < 0.05)$, indicating antagonistic effects (Table 1). Quite similar effects were observed in A-549 and Lu-99 cells (Table 1, isobolograms not shown).

Sequential exposure to pemetrexed for 24 h followed by docetaxel for 24 h

Figure 4b shows isobolograms of SBC-5 cells exposed first to pemetrexed and then to docetaxel. The combined data points fell in the area of supraadditivity. The mean values of the observed data (0.46) were smaller than those
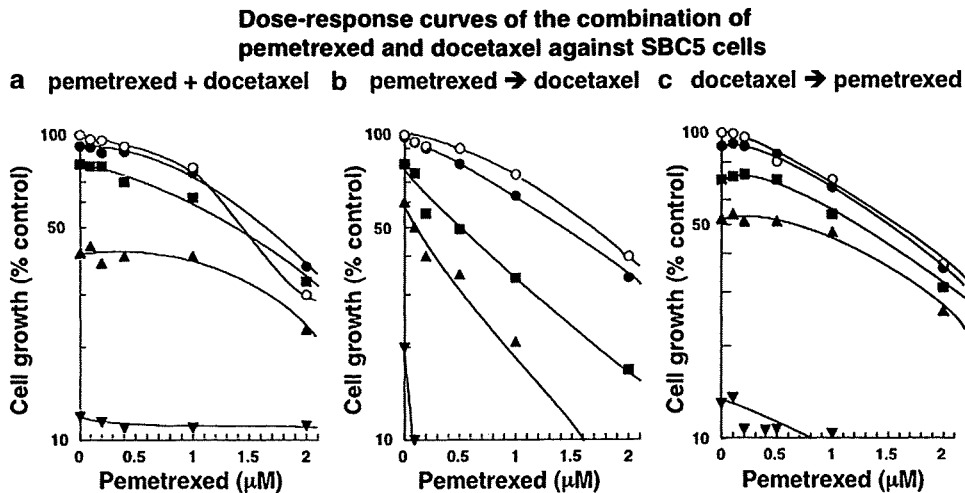
Dose-response curves of the combination of pemetrexed and docetaxel against SBC5 cells

a pemetrexed + docetaxel   b pemetrexed → docetaxel   c docetaxel → pemetrexed

Fig. 3 Schedule dependence of the interaction between docetaxel and pemetrexed in SBC-5 cells. Cells were exposed to these two drugs simultaneously for 24 h (a), pemetrexed first for 24 h followed by docetaxel for 24 h (b), and vice versa (c). The cell number after 5 days was measured using the MTT assay and was plotted as a percentage of the control (cells not exposed to drugs). The concentrations of docetaxel are shown on the abscissa. The concentrations of pemetrexed were 0 (*open circle*), 0.2 (*filled circle*), 0.5 (*filled square*), 1.0 (*filled triangle*) and 2.0 (*filled inverted triangle*) μM, respectively. Data are mean values for three independent experiments; SE was < 25%

Isobolograms of the combination of pemetrexed and docetaxel against SBC5 cells

a pemetrexed + docetaxel   b pemetrexed → docetaxel   c docetaxel → pemetrexed
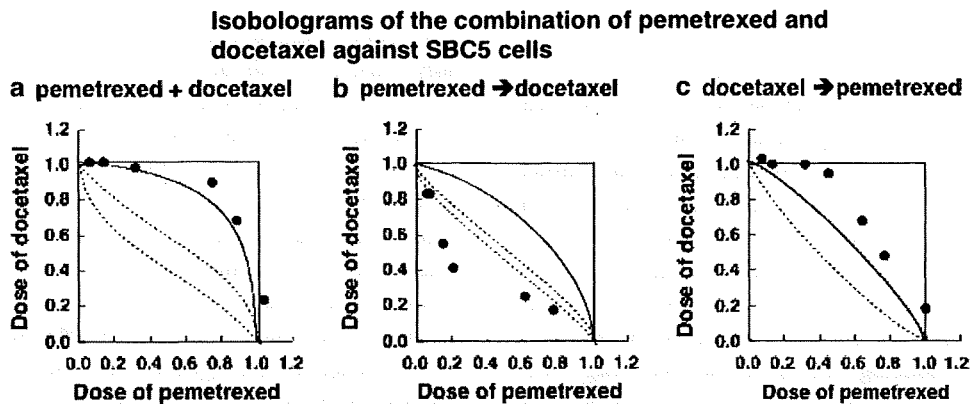

Fig. 4 Isobolograms of simultaneous exposure to docetaxel and pemetrexed for 24 h in SBC-5 cells (a). The combined data points fell in the areas of subadditivity and protection. Data are mean values for at least three independent experiments; SE was <25%. Isobolograms of sequential exposure to pemetrexed (24 h) followed by docetaxel (24 h) in SBC-5 cells (b). All data points of the combinations fell in the area of supraadditivity. Data are mean values for at least three independent experiments; SE was <20%. Isobolograms of sequential exposure to docetaxel (24 h) followed by pemetrexed (24 h) in SBC-5 cells (c). All data points of the combinations fell in the areas of subadditivity and protection. Data are mean values for at least three independent experiments; SE was <25%

of the predicted minimum values (0.60) (Table 1). The difference was significant ($P < 0.05$), indicating synergistic effects. Quite similar effects were observed in Lu-99 cells (Table 1, isobolograms not shown), while additive effects were observed in A-549 cells (Table 1, isobolograms not shown).

Sequential exposure to docetaxel for 24 h followed by pemetrexed for 24 h

Figure 4c shows isobolograms of SBC-5 cells exposed first to docetaxel, followed by pemetrexed. The combined data points mainly fell in the area of subadditivity. The mean values of the observed data were larger than those of the

predicted maximum values ($P < 0.02$) (Table 1), indicating antagonistic effects. For A-549 and Lu-99 cells, most combined data points fell within the envelope of additivity and the mean values of the observed data were between those of the predicted minimum and maximum values (Table 1, isobolograms not shown), indicating an additive effect of this schedule.

Simultaneous exposure to pemetrexed and docetaxel for 5 days

For all three cell lines, combined data points fell in the areas of subadditivity and protection, indicating antagonistic effects (Table 1, isobolograms not shown).

Table 1 Mean values of observed data, predicted minimum, and predicted maximum of pemetrexed and docetaxel in combination at IC_{50} level

Schedule	Cell line	n^a	Observed data	Predicted min.[b]	Predicted max.[c]	Effects
Pemetrexed + docetaxel (24 h)	A-549	8	0.72	0.31	0.55	Antagonism ($P < 0.02$)
	Lu-99	6	>1.0	0.41	0.62	Antagonism ($P < 0.05$)
	SBC-5	6	0.71	0.33	0.60	Antagonism ($P < 0.05$)
Pemetrexed (24 h) → docetaxel (24 h)	A-549	7	0.63	0.31	0.92	Additive
	Lu-99	7	0.29	0.50	0.67	Synergism ($P < 0.02$)
	SBC-5	7	0.46	0.60	0.82	Synergism ($P < 0.02$)
Docetaxel (24 h) → pemetrexed (24 h)	A-549	8	0.64	0.32	0.86	Additive
	Lu-99	8	0.63	0.32	0.85	Additive
	SBC-5	7	0.87	0.36	0.70	Antagonism ($P < 0.02$)
Pemetrexed + docetaxel (5 day)	A-549	6	0.79	0.51	0.68	Antagonism ($P < 0.05$)
	Lu-99	6	0.96	0.45	0.62	Antagonism ($P < 0.05$)
	SBC-5	4	0.73	0.20	0.57	Antagonism ($P < 0.05$)

[a] Number of data points

[b] Predicted minimum value for an additive effect

[c] Predicted maximum value for an additive effect

Cell cycle analysis

The isobologram analysis revealed that pemetrexed and docetaxel had a synergistic effect on two of the three lung cancer cell lines when sequentially administered with pemetrexed first and followed by docetaxel. In contrast, either simultaneous exposure or sequential addition in the reversed order (docetaxel to pemetrexed) resulted in antagonistic or additive effects. We confirmed these results by calculating the size of sub-G1 fractions, which correspond to apoptotic populations, on flow cytometry. As shown in Fig. 5, apoptosis-inducing effects of the two drugs were strongest when cells were exposed to pemetrexed first and followed by docetaxel. In contrast, the cytotoxic effects of docetaxel were significantly suppressed when pemetrexed was added simultaneously or afterward. These data are fully consistent with the results of isobologram analysis.

Cell cycle analysis also provided a clue to understand the mechanisms underlying this observation. Pemetrexed alone induced cell cycle arrest in late G1 to early S phase in SBC-5 cells (see Fig. 6 for representative results, and Table 2 for quantification and statistical analysis of three independent experiments). Docetaxel alone caused the loss of mitotic fractions along with massive apoptosis at a relatively low concentration (1.5 nM). When SBC-5 cells were exposed to both agents simultaneously, the cell cycle pattern was between the patterns of single-agent exposure, and the size of sub-G1 fractions was substantially
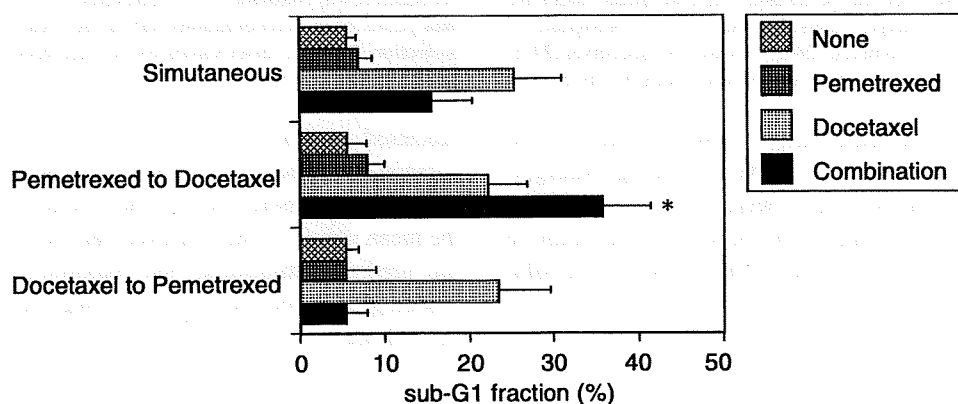

Fig. 5 SBC-5 cells were cultured in the absence (None) or presence of either 5.0 μM pemetrexed (Pemetrexed) or 1.5 nM docetaxel (Docetaxel) alone for 24 h; or in the presence of both drugs for 24 h (Simultaneous); or treated with pemetrexed for 24 h, followed by docetaxel for 24 h (Pemetrexed to Docetaxel); or treated with docetaxel for 24 h, followed by pemetrexed for 24 h (Docetaxel to Pemetrexed). After 72 h, DNA histograms were obtained to calculate the size of sub-G1 fractions as described in "Materials and methods". Data shown are the means ± SD of three independent experiments. The statistical difference was determined by one-way ANOVA with Bonferroni multiple comparison test. An *asterisk* denotes $P < 0.01$

Fig. 6 Cell cycle analysis of SBC-5 cells treated with docetaxel and pemetrexed. *Left column* SBC-5 cells were treated with no drug, 5.0 μM pemetrexed, 1.5 nM docetaxel, or both drug simultaneously for 24 h. *Middle column* SBC-5 cells were treated with 5.0 μM pemetrexed for 24 h, followed by 1.5 nM docetaxel for 24 h. *Right column* SBC-5 cells were treated with 1.5 nM docetaxel for 24 h, followed by 5.0 μM pemetrexed for 24 h. Cells were harvested at 72 h and DNA histogram was obtained as described in "Materials and methods"
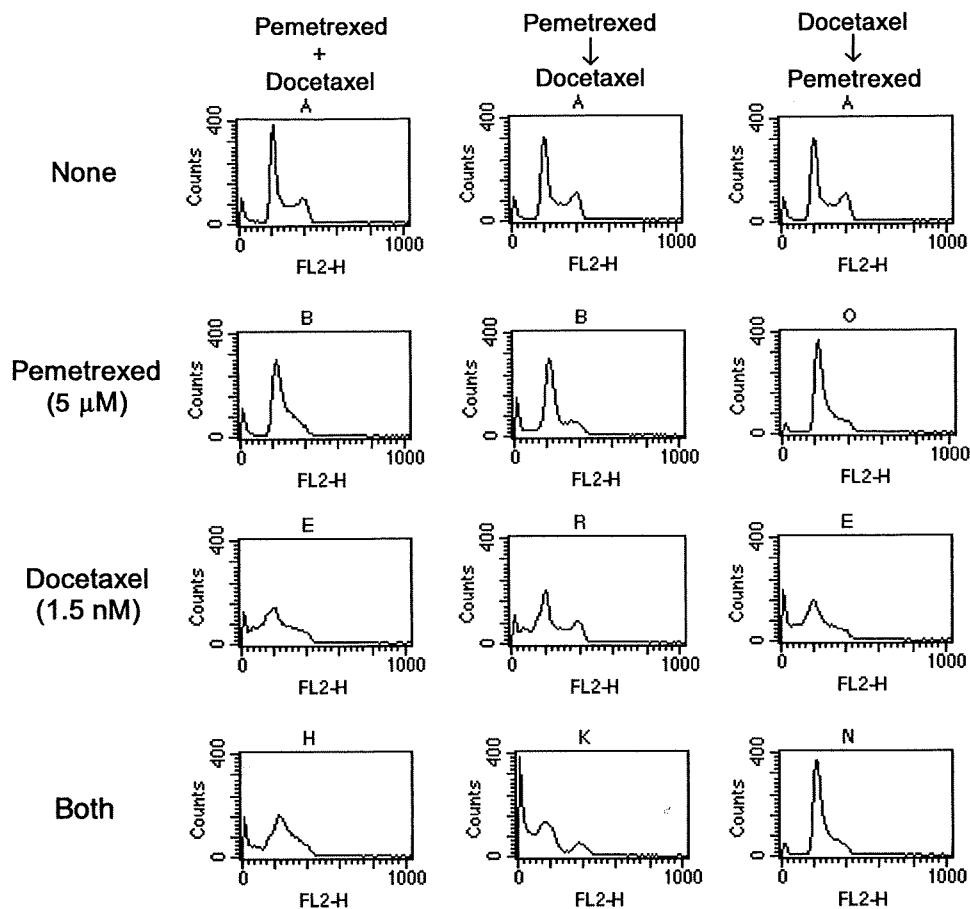
reduced. When SBC-5 cells were treated with docetaxel first and followed by pemetrexed, the cell cycle profile was almost identical to that of single exposure to pemetrexed, suggesting that the cell cycle effect of pemetrexed is dominant over that of docetaxel. As a result, the apoptosis-inducing effect of docetaxel was almost completely cancelled in the presence of pemetrexed. In contrast, when SBC-5 cells were treated with pemetrexed first and followed by docetaxel, the proportion of cells in sub-G1 phase was larger than that of cells treated with either pemetrexed or docetaxel alone. This was accompanied by a decrease in S-phase cells. Overall, the results of cell cycle analysis are fully consistent with those of isobologram analysis, and provide the molecular basis of the sequence-dependent differences in cytotoxic interactions between the two agents.

Discussion

In this study, we investigated the effects of pemetrexed in combination with docetaxel on lung cancer cell lines to determine the optimal schedule for this combination. Analysis of the drug–drug interaction effects was carried out using the isobologram method of Steel and Peckham [18], which provides a fundamental basis for assessing whether cytotoxicity induced by combinations of anticancer agents is greater, equal to, or smaller than would have been expected for the individual agents.

We demonstrated that a cytotoxic interaction between pemetrexed and docetaxel is schedule-dependent. Simultaneous exposure to pemetrexed and docetaxel for 24 h and 5 days showed antagonistic effects in all cell lines studied. Sequential exposure to pemetrexed for 24 h followed by docetaxel for 24 h showed synergistic effects in Lu-99 and SBC-5 cells, while it showed additive effects in A-549 cells. Sequential exposure to docetaxel followed by pemetrexed showed additive effects in A-549 and Lu-99 cells, but antagonistic effects in SBC-5 cells. We also used SW620 colon cancer cells for the study, and the combined effects for these schedules were quite the same as those of SBC-5 cells (data not shown).

These findings suggest that the sequential administration of pemetrexed followed by docetaxel may be more cytotoxic to cancer cells and optimal for this combination, while the simultaneous administration of pemetrexed and docetaxel may be less cytotoxic and suboptimal. It should be noted that the sequential administration of pemetrexed

Table 2 Effects of pemetrexed and docetaxel on cell cycle distribution of SBC-5 cells

Schedule	Pemetrexed + Docetaxel (%)	Pemetrexed ↓ Docetaxel (%)	Docetaxel ↓ Pemetrexed (%)
None			
Sub-G1	5.4	4.7	4.7
G1	48.4	51.3	51.3
S	24.9	22.3	22.3
G2/M	21.3	21.7	21.7
Pemetrexed (5 μM)			
Sub-G1	5.5	9.9	2.2
G1	62.8	61.6	68.2
S	28.4	18.1	20.0
G2/M	3.3	10.4	9.6
Docetaxel (1.5 nM)			
Sub-G1	25.2	17.6	21.3
G1	42.8	4.7	50.7
S	27.1	20.0	18.3
G2/M	4.9	17.7	9.7
Both			
Sub-G1	14.6	36.0	2.3
G1	52.1	40.1	66.4
S	22.7	12.2	26.0
G2/M	3.6	11.7	5.3

The proportion of cells in each phase of the cell cycle was calculated with the ModFitLT 2.0 program

followed by docetaxel might be more toxic for normal cells. Since, however, toxicity profiles of both agents are different, increasing overlapping toxicity would likely be mild.

Previously, we evaluated the cytotoxic effects of pemetrexed in combination with paclitaxel in vitro using A-549 cells, breast cancer MCF7, ovarian cancer PA1, and colon cancer WiDr cells in vitro [17]. The results were similar to those of the present study. Although slight differences are present, this would be due to the very strict definitions of synergism and antagonism in the isobologram method (Steel and Peckham). Our previous and present findings suggest that the simultaneous administration of pemetrexed and taxanes is less cytotoxic than the sequential administration of pemetrexed followed by taxanes, and latter schedule should be assessed in clinical trials for the treatment of lung cancer and other solid tumors.

In general, it is difficult to clarify the mechanisms underlying the cytotoxic effects of drug combinations. In this study, however, cell cycle analysis provided a clue to the molecular basis of schedule-dependent synergism and antagonism. The exposure of SBC-5 cells to pemetrexed led to synchronization of most cells that were in late G1 phase to the early S phase of the cell cycle, during which

cells are relatively insensitive to docetaxel. This may explain the antagonistic effects of the simultaneous addition of the two agents. In the case of sequential exposure to docetaxel followed by pemetrexed, the cell cycle pattern was almost identical to that of cells treated with pemetrexed alone. This suggests that the cell cycle effect of docetaxel is transient and overcome by the addition of pemetrexed, which results in the abrogation of its cytotoxicity.

In contrast, the sequential exposure to pemetrexed followed by docetaxel produced a striking increase in apoptotic cells along with a decrease in cells in S phase. The effect of docetaxel on S phase cells no longer in pemetrexed-induced cell cycle arrest may cause the synergistic cytotoxicity. The decrease in S phase is compatible with this notion. However, the mechanisms underlying the cytotoxic effects of pemetrexed and docetaxel are still not well understood. The possibility that the drug interactions are due to some unknown mechanism related to complex perturbations of biochemical processes cannot be excluded.

In conclusion, our data show that the antitumor activity of pemetrexed and docetaxel is schedule-dependent. Sequential exposure to pemetrexed followed by docetaxel tended to produce synergistic effects, and would therefore be a suitable schedule, whereas simultaneous exposure to the two agents had antagonistic effects, and may be suboptimal. However, the question of how far these results can be applied in the treatment of patients remains unanswered. Further clinical studies are necessary to clarify whether the therapy sequence alters the antitumor effect and the toxicity of this combination. Our findings provide preclinical rationale for a novel, mechanism-based, therapeutic strategy to be tested in lung cancer patients.

Conflict of interest statement None.

References

1. Shepherd FA (2000) Chemotherapy for advanced non-small-cell lung cancer: modest progress, many choices. J Clin Oncol 18(21 Suppl):35S–38S
2. Non-Small Cell Lung Cancer Collaborative Group (1995) Chemotherapy in non-small cell lung cancer: a meta analysis using updated data on individual patients from 52 randomized trials. Br J Cancer 311:899–909
3. Shepherd FA, Carney DN (2000) Treatment of non-small cell lung cancer: chemotherapy. In: Hansen HH (ed) Textbook of lung cancer. Martin Dunitz, London, pp 213–242
4. Cullen M (2006) Second-line treatment options in advanced non-small cell lung cancer: current status. Semin Oncol 33(1 Suppl 1):S3–S8

5. Massarelli E, Herbst RS (2006) Use of novel second-line targeted therapies in non-small cell lung cancer. Semin Oncol 33(1 Suppl 1):S9–S16

6. Govindan R, Page N, Morgensztern D et al (2006) Changing epidemiology of small-cell lung cancer in the United States over the last 30 years: analysis of the surveillance, epidemiologic, and end results database. J Clin Oncol 24:4539–4544

7. Rosti G, Carminati O, Monti M et al (2006) Chemotherapy advances in small cell lung cancer. Ann Oncol Suppl 5:99–102

8. Socinski MA, Weissman CH, Hart LL et al (2005) A randomized phase II trial of pametrexed (P) plus cisplatin (cis) or carboplatin (carbo) in extensive stage small cell lung cancer (ES-SCLC). Proc ASCO (a 7165)

9. Gronberg BH, Bremnes RM, Aasebo U et al, on behalf of the Norwegian Lung Cancer Study Group (2008) A prospective phase II study: High-dose pemetrexed as second-line chemotherapy in small-cell lung cancer. Lung Cancer Jun 5 [Epub ahead of print]

10. Khan RA, Hahn B (2008) Phase II trial of weekly topotecan with docetaxel in recurrent small cell lung cancer. Proc ASCO (a19111)

11. Adjei AA (2004) Pemetrexed (ALIMTA), a novel multitargeted antineoplastic agent. Clin Cancer Res 10:4276S–4280S

12. Hanna N, Shepherd FA, Fossella FV et al (2004) Randomized phase III trial of pemetrexed versus docetaxel in patients with non-small-cell lung cancer previously treated with chemotherapy. J Clin Oncol 22:1589–1597

13. Shih C, Chen VJ, Gossett LS et al (1997) LY231514, a pyrrolo[2, 3-d]pyrimidine-based antifolate that inhibits multiple folate-requiring enzymes. Cancer Res 57:1116–1123

14. Tonkinson JL, Marder P, Andis SL et al (1997) Cell cycle effects of antifolate antimetabolites: implications for cytotoxicity and cytostasis. Cancer Chemother Pharmacol 39:521–531

15. Jones SE, Erban J, Overmoyer B et al (2005) Randomized phase III study of docetaxel compared with paclitaxel in metastatic breast cancer. J Clin Oncol 23:5542–5551

16. Gligorov J, Lotz JP (2004) Preclinical pharmacology of the taxanes: implications of the differences. Oncologist 9(Suppl 2):3–8

17. Kano Y, Akutsu M, Tsunoda S et al (2004) Schedule-dependent synergism and antagonism between pemetrexed and paclitaxel in human carcinoma cell lines in vitro. Cancer Chemother Pharmacol 54:505–513

18. Steel GG, Peckham MJ (1979) Exploitable mechanisms in combined radiotherapy-chemotherapy: the concept of additivity. Int J Radiat Oncol Biol Phys 5:85–91

19. Kano Y, Sakamoto S, Kasahara T et al (1991) In vitro effects of amsacrine in combination with other anticancer agents. Leukemia Res 15:1059–1064

20. Kano Y, Ohnuma T, Okano T et al (1988) Effects of vincristine in combination with methotrexate and other antitumor agents in human acute lymphoblastic leukemia cells in culture. Cancer Res 48:351–356

21. Kano Y, Suzuki K, Akutsu M et al (1992) Effects of CPT-11 in combination with other anticancer agents in culture. Int J Cancer 50:604–610

22. Kano Y, Akutsu M, Tsunoda S et al (1994) In vitro schedule-dependent interaction between and SN-38 (the active metabolite of irinotecan) in human carcinoma cell lines. Cancer Chemother Pharmacol 42:91–98

23. Kikuchi J, Shimizu R, Wada T et al (2007) E2F-6 suppresses growth-associated apoptosis of human hematopoietic progenitor cells by counteracting proapoptotic activity of E2F-1. Stem Cells 25:2439–2447

The juxtamembrane domain in ETV6/FLT3 is critical for PIM-1 up-regulation and cell proliferation

Hoang Anh Vu [a,b], Phan Thi Xinh [b], Yasuhiko Kano [d], Katsushi Tokunaga [c], Yuko Sato [b,*]

[a] Consolidated Research Institute for Advanced Science and Medical Care (ASMeW), Waseda University, Tokyo, Japan
[b] Division of Ultrafine Structure, Department of Pathology, Research Institute of International Medical Center of Japan, Toyama 1-21-1, Shinjuku-ku, Tokyo 162-8655, Japan
[c] Department of Human Genetics, School of International Health, Graduate School of Medicine, The University of Tokyo, Tokyo, Japan
[d] Division of Hematology, Department of Hematology and Medical Oncology, Tochigi Cancer Center, Tochigi, Japan

ARTICLE INFO

ABSTRACT

We recently reported that the ETV6/FLT3 fusion protein conferred interleukin-3-independent growth on Ba/F3 cells. The present study has been conducted to assess role of the juxtamembrane domain of FLT3 for signal transduction and cell transformation. The wild-type ETV6/FLT3 fusion protein in transfected cells was a constitutively activated tyrosine kinase that led to up-regulation of PIM-1 and activations of STAT5, AKT, and MAPK. Deletion of the juxtamembrane domain abrogated interleukin-3-independent growth of the transfected cells and PIM-1 up-regulation, whereas it retained compatible levels of phosphorylations of STAT5, AKT, and MAPK. Further deletion of N-terminal region of the tyrosine kinase I domain of FLT3 completely abolished these phosphorylations. Our data indicate that the juxtamembrane domain of FLT3 in ETV6/FLT3 fusion protein is critical for cell proliferation and PIM-1 up-regulation that might be independent of a requirement for signaling through STAT5, MAPK, and AKT pathways.

© 2009 Elsevier Inc. All rights reserved.

The *FLT3* (FMS-like tyrosine kinase 3) gene, a member of the receptor tyrosine kinase (RTK) subclass III family genes including *FMS*, *KIT*, and *PDGFR* [1,2], is characterized by an extracellular region consisting of five immunoglobulin-like domains, a transmembrane region, a cytoplasmic juxtamembrane (JM) domain, and two cytoplasmic TK domains linked by a kinase insert [3].

Although FLT3 activation has been known to result in the autophosphorylation of its tyrosine residues, very little is known about the contribution of each tyrosine residues to FLT3 signal transduction. Recently, four tyrosine-phosphorylation sites (Y572, Y589, Y591, and Y599) have been identified in the JM domain of wild-type (WT-) FLT3 after stimulation with ligand, where phosphorylated tyrosines 589 and 599 are docking sites for signaling intermediates including Src family kinases and protein tyrosine phosphatase SHP2 [4]. It was also reported that tyrosines 579 and 581 of the JM domain of PDGFRB determined myeloproliferative phenotype in mouse [5], suggesting that the JM domain of RTK subclass III family genes not only has an autoinhibitory effect on the catalytic activity of the kinase domain but also might play a more active role in leukemogenesis.

FLT3 is one of the most frequently mutated genes in hematologic malignancies [6]. The most common mutation of *FLT3* is an internal tandem duplication in exons 14 and 15 of the JM domain (FLT3-ITD) [7,8], whereas other mutations such as point mutations at and around codon 835 of exon 20 (FLT3-TKD) [9,10], or point mutations in the JM domain (FLT3-JM-PM) [11] have also been found. Mutations promote constitutive phosphorylation of the receptor and ligand-independent cell growth [11,12]. Unlike WT-FLT3, five phosphorylated tyrosines (Y591, Y726, Y842, Y955, and Y969) were identified in FLT3-ITD, among which four belongs to the TK domain and only one (Y591) to the JM domain [13]. The combination of Y589 and Y591 in FLT3-ITD is required for activation of signal transducer and activator of transcription 5 (STAT5), which was not observed after activation of WT-FLT3. In contrast to FLT3-ITD, FLT3-TKD was unable to activate STAT5 as well as its downstream target genes PIM-2 and CIS [12], nevertheless FLT3-JM-PM induced STAT5 activation with a lower level compared with that of FLT3-ITD [11]. However, there are controversial data regarding signaling pathways of mutant FLT3: Some group reported that STAT5 was activated by WT-FLT3 and FLT3-TKD [11,14,15], whereas others failed to show such an activation [16]. The different observations may be due to different cell culture systems that they employed. More information about deregulated signaling of mutated FLT3 is needed to understand the molecular pathogenesis in FLT3-related leukemias.

We have previously identified several types of ETV6/FLT3 (EF) fusion proteins in a patient with myeloproliferative disorder (MPD) and a t(12;13)(p13;q12) translocation [17]. Intrigued by the observation that only the EF1 isoform which retained the JM

* Corresponding author. Fax: +81 3 5273 8603.
E-mail address: ysato@ri.imcj.go.jp (Y. Sato).

domain as well as the two intact TK domains of FLT3, but not the EF7 isoform which lacked the JM domain and N-terminal region of the TK1 domain of FLT3, induced growth factor-independent cell proliferation, we sought to identify the corresponding residues required for signal transduction and cell transformation.

Materials and methods

Plasmid constructs. WT-*ETV6/FLT3* cDNAs, *EF1*, and *EF7*, were constructed from the patient sample by PCR and were ligated into the BamHI site of pcDNA3.1(+) vector (Invitrogen, Carlsbad, CA, USA) as described previously [17]. Subsequently, plasmid pcDNA3.1(+)-*EF1* was used as a template for site-directed mutagenesis. Five tyrosine to phenylalanine substitutions (Y589F, Y591F, Y597F, Y599F, and Y630F), deletion of the JM domain (Δ30, deletion from Ser 574 through Trp 603), and deletion of the JM domain plus N-terminal region of the TK1 domain (Δ74, deletion from Ser 574 through Lys 647) were generated using the QuickChange XL site-directed mutagenesis kit (Stratagene, La Jolla, CA, USA) according to the manufacturer's instructions. The Δ30 deletion was created using 5'-CGGGCTGCATAGGGAAGGGGAG-TTTCCAAGAGAAAATTTAG-3' and 5'-CTAAATTTTCTCTTGGAAACTCCCCTTCC-CTATGCAGCCCG-3' as mutagenic primers. The oligonucleotides used for the Δ74 deletion were 5'-GGGCTGCATAGGGAAGGGGAAAAAGCAGACAGCTCTG-3' and 5'-CAGA-GCTGTCTGCTTTTTCCCCTTCCCTATGCAGCCC-3'. All mutations were confirmed by DNA sequencing.

Cell culture, transfections, and proliferation assays. Ba/F3 cells and 32D cells were stably transfected with each of the constructs, using Lipofectamine (Invitrogen) as described previously [17]. Cells were maintained in RPMI 1640 medium supplemented with 10% fetal bovine serum (FBS) and 1 ng/ml of recombinant mouse interleukin 3 (IL-3; R&D Systems, Minneapolis, MN). PKC412 (kindly provided by Novartis Pharma AG, Basel, Switzerland) was dissolved in dimethyl sulfoxide (DMSO) as stock solution at 1 mM and stored at −20 °C. For proliferation assays, cells were washed four times with PBS and then 5×10^3 cells per well were seeded in quadruplicate in 96-well plates, in 100 μl of culture media in the presence of various concentrations of IL-3 or PKC412 with final concentration of DMSO <0.1%. After incubation for 72 h, 10 μl of TetraColor ONE reagent containing tetrazolium monosodium salt (Seikagaku Corporation, Tokyo, Japan) was added to each well and cells were incubated for additional 4 h. Absorbance at 450 nm was measured with the Biotrack II plate reader (Amersham Biosciences, Uppsia, Sweden). Results were enumerated as the percentage of the values measured when cells were grown in the presence of 1 ng/ml IL-3.

Antibodies. The following antibodies were obtained from Santa Cruz Biotechnology (Santa Cruz, CA, USA): Flt3/Flk2 (S-18: sc-480), Stat5 (C-17: sc-835), Pim-1 (12H8: sc-13513), Akt1 (C-20: sc-1618), ERK1 (K-23: sc-94), anti-rabbit IgG- HRP (sc-2317), anti-mouse IgG-HRP (sc-2031), and anti-goat IgG-HRP (sc-2033). Anti-phosphotyrosine 4G10 was from Upstate Biotechnology (Lake Placid, NY, USA), anti-actin (A2066) from Sigma (Saint Louis, MO, USA), phospho-Stat5 (Tyr694), phospho-p44/42 Map kinase (Thr202/Tyr204), and phospho-Akt (Ser473) antibodies from Cell Signaling Technology (Danvers, MA, USA).

Western blot analysis and immunoprecipitation. Stably transfected cells were grown to a density of approximately 1×10^6/ml in the presence of IL-3. Cells were washed twice with PBS and starved of IL-3 by culturing in only media overnight. *EF1*-transfected cells were incubated with different concentrations of PKC412 for additional 4 h. Subsequently, cells were washed once with ice-cold PBS and total cell lysates were isolated using RIPA buffer (Santa Cruz Biotechnology) according to the manufacturer's instructions. Immunoprecipitation and immunoblotting using a chemiluminescence technique were performed as described previously [17].

Results and discussion

Lack of the JM domain of FLT3 in EF1 abrogated cell transformation ability, despite retaining high level of its autophosphorylation on tyrosine

Since only EF1, but not EF7 which lacked the JM domain and N-terminal region of the TK1 domain of FLT3, induced growth factor-independent cell proliferation [17], we hypothesized that tyrosine residues in the JM domain and TK1 domain of FLT3 in EF1 oncoprotein might have an important role in pathogenesis of MPD. As an initial study based on this hypothesis, we generated five tyrosine to phenylalanine mutants (Y589F, Y591F, Y597F, Y599F, and Y630F) and two deletion mutants (Δ30 and Δ74) from EF1 (Fig. 1). Although each substitution mutant impaired the growth of Ba/F3 cells in response to IL-3, they were ultimately able to transform Ba/F3 cells to IL-3 independence (Fig. 2A) and each of them demonstrated constitutive autophosphorylation of EF in Ba/F3 cells (Fig. 2B), suggesting that not any single tyrosine residue was fully responsible for IL-3-independent cell growth. Ba/F3-Δ30 cells, like Ba/F3-Δ74 cells and Ba/F3-EF7 cells, could not grow in IL-3-free media, and all cells died within 3 days. To our surprise, in contrast to a dramatically reduced IL-3-independent cell growth, the deletion of the JM domain (Δ30) did not affect on autophosphorylation of EF (Fig. 2B). Similar observation was found in transfected 32D cells (data not shown). The finding proposes a very important role of the JM domain of FLT3 for cell transformation, and suggests that full transformation of Ba/F3 cells may require other factor(s) besides kinase activity. On the other hand, the N-terminal region of the TK1 domain, which contains the single tyrosine 630, is expected to possess kinase activity because its deletion (Δ74) completely abolished both IL-3-independent cell growth and autophosphorylation of the fusion protein (Fig. 2A and B). Since it was showed that phosphorylation status of tyrosine 630 in FLT3-ITD was indeterminate using *in vitro* mapping of tyrosine-phosphorylation sites [13], whether phosphorylation status of tyrosine 630 in the EF1 fusion protein is different from its status in FLT3-ITD requires further experiment to answer. The residual phosphorylation observed in Ba/F3-Y630F cells could be due to the autophosphorylation of tyrosines 589, 591, and 599 of the JM domain [4,13].

Activation of STAT5 and expression of PIM-1 by WT-EF1 and related mutants

STAT5 is a member of a family of latent cytoplasmic transcription factors which are involved in cytokine, hormone, and growth factor signal transduction [18]. Even though activation of STAT5 was believed to play a major role in FLT3-ITD-induced autonomous cell growth, there were controversial reports on the role of tyrosine residues in the JM of FLT3-ITD for the activation. Murata et al. [19] and Rocnik et al. [13] clearly showed that tyrosines 589 and 591 are required for STAT5 activation, whereas Kiyoi et al. observed constitutively activated STAT5 in deletion mutant encompassing residues 589–599 of FLT3 [20]. As shown in Fig. 3A, phosphorylation of STAT5 on tyrosine was found in Ba/F3-EF1 cells. Although each of the substitutions Y591F, Y597F, and Y599F in the JM domain reduced STAT5 phosphorylation intensity, the Y589F retained this phosphorylation. Again, in contrast to severe reduction in cell proliferation, deletion of the JM domain (Δ30) that contains these four tyrosine residues showed a somewhat stronger level of STAT5 activation than that of EF1. Further deletion of N-terminal part of the TK1 domain of FLT3 (Δ74) did abrogate this phosphorylation and very weak STAT5 phosphorylation was observed in Ba/F3-
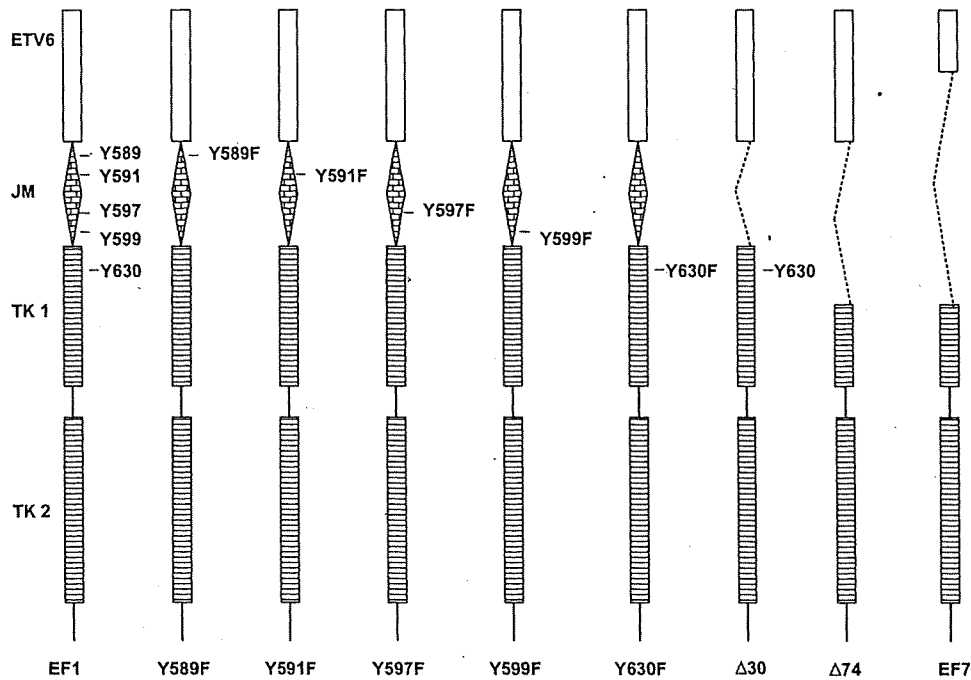
Fig. 1. Schematic structures of the wild-type EF1 and its mutants. The N-terminal ETV6 portion, depicted by an empty box, remains unchanged in EF1 and its mutant proteins. Tyrosine residues in the FLT3 portion are indicated as "Y" and are numbered according to the wild-type FLT3 sequences. In the Δ30 and Δ74 constructs, Ser 574 through Trp 603 and Ser 574 through Lys 647 are deleted, respectively. In the mutants with tyrosine to phenylalanine substitution, each of the five tyrosine residues is mutated. EF7 is also illustrated to show difference in the ETV6 portion between Δ74 and EF7.
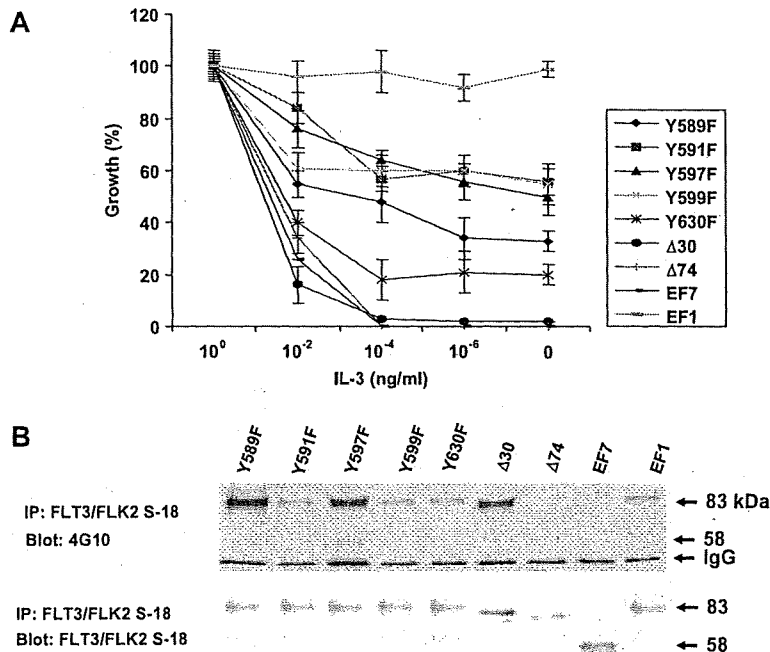

Fig. 2. Full transformation of Ba/F3 cells requires other factor(s) than EF kinase activity. (A) Transforming activities of EF1 and its mutants. 5 × 10³ Ba/F3 cells transfected with wild-type EF1 or its variants were grown in the presence of various concentrations of IL-3 in each well of 96-well plates. After 72 h, TetraColor ONE cell proliferation assays were performed to measure the cell growth. Results are expressed as the percentage of the values measured when cells were grown with 1 ng/ml IL-3. The data presented are the average of three separate experiments. (B) Autophosphorylation of EF1 and its mutants in Ba/F3 cells. Transfected Ba/F3 cells were starved of IL-3 overnight. Cell lysates were immunoprecipitated with an antibody against FLT3, followed by immunoblot analysis with an anti-phosphotyrosine antibody, 4G10.
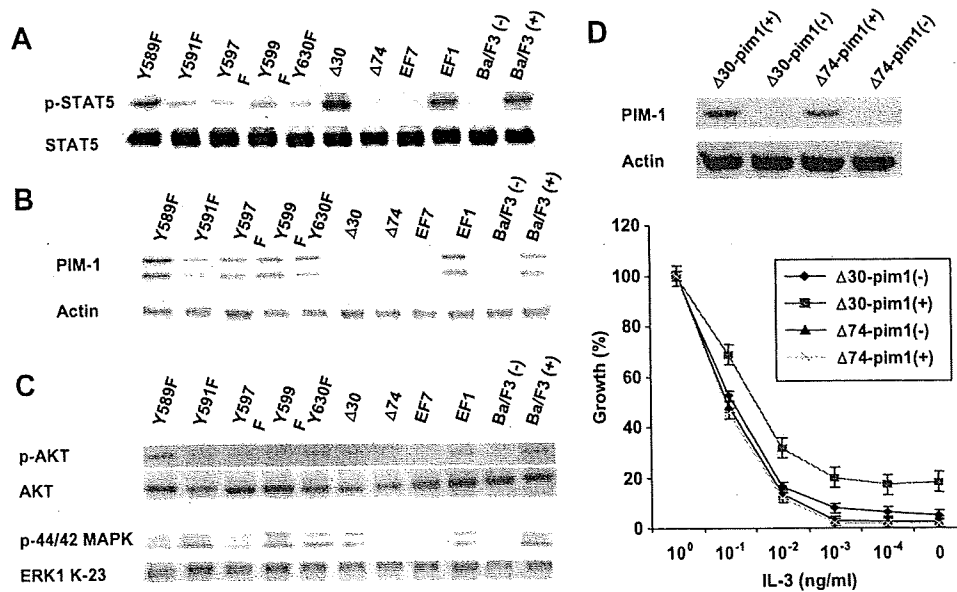
Fig. 3. Signal transduction in Ba/F3 cells expressing EF1 and its mutant proteins. (A) Transfected Ba/F3 cells were starved of IL-3 overnight. Cell lysates were immunoblotted with phospho-STAT5 antibody or STAT5 antibody. (B) PIM-1 expression was examined by immunoblot analysis of total cell lysates using an anti-PIM-1 antibody, and equivalent protein loading was indicated by an anti-actin antibody. PIM-1 is expressed as two isoforms of 33 and 44 kDa. (C) Cell lysates were immunoblotted with phospho-AKT antibody or AKT antibody (top panels) and phospho-MAPK antibody or ERK antibody (bottom panels). Ba/F3(−), parental Ba/F3 cells starved of IL-3 overnight; Ba/F3(+), parental Ba/F3 cells cultured in media with IL-3. (D) Ba/F3 cells expressing Δ30 or Δ74 were co-transfected with PIM-1 construct. Western blot was performed after cells were starved of IL-3 overnight. For proliferation assay, 5×10^3 cells were grown in the presence of various concentrations of IL-3 in each well of 96-well plates. After 72 h, TetraColor ONE cell proliferation assays were performed to measure the cell growth.

Y630F cells. We also observed the same phenomena with transfected 32D cells (data not shown). It is likely that, unlike FLT3-ITD, the EF1 fusion protein might not utilize the JM domain alone for STAT5 activation. Instead, our results point out that the N-terminal region of TKI domain containing the tyrosine 630 is required for STAT5 activation. In fact, we further generated a construct lacking only the N-terminal region of TKI domain from EF1 (deletion of Glu 604 through Lys 647), and found that the stable Ba/F3 cells expressing this construct failed to activate STAT5 in the absence of IL-3 (data not shown). However, substitution of tyrosine 630 in Δ30 construct by phenylalanine retained STAT5 activation in Ba/F3 cells (data not shown), indicating that the tyrosine 630 alone is not fully responsible for STAT5 activation.

Although precise signaling pathways critical for transformation of Ba/F3 ·cells are not thoroughly understood, PIM-1 may be an important downstream target gene of STAT5, which is involved in constitutively activated FLT3 signaling pathways [21]. Up-regulation of PIM-1, observed in AML samples with FLT3-ITD [21], mediates the anti-apoptotic function of the mutant FLT3 signaling via the phosphorylation of BAD [22]. However, how the mutant FLT3 up-regulated PIM-1 have not been addressed in these studies. As shown in Fig. 3B, PIM-1 was overexpressed in Ba/F3-EF1 cells. In accordance with cell proliferation ability, PIM-1 expression was undetectable in Ba/F3 cells expressing the deletion mutants (Figs. 2A and 3B). To further demonstrate that PIM-1 contributes to factor-independent cell growth, we exogenously introduced PIM-1 in Ba/F3 cells expressing the deletion mutants to see whether they gain factor-independency. As expected, expression of PIM-1 in Δ30-expressing cells led to a significant increase in cell growth in the absence of IL-3 (18.2% increase), whereas it had no affect in Δ74-expressing cells (Fig. 3D). On the other hand, the fact that the Y589F mutant that showed high level of PIM-1 expression exhibited much lower cell growth than EF1 suggested that PIM-1 might need to cooperate with other factors to fully transform cells,

such as Src family kinases and protein tyrosine phosphatase SHP2 [4], or c-myc [23], which might be retained in Δ30-expressing cells but silenced in Δ74-expressing cells. Importantly, our data strongly suggests that up-regulation of PIM-1 requires other factor(s) besides the activated STAT5 because nearly undetectable expression of PIM-1 was observed in Δ30-expressing cells which showed strong STAT5 activation (Fig. 3A and 3B). It is possible that, even though deletion of the JM domain of FLT3 retained STAT5 activation, lack of the JM domain might abolish activation of other factor(s) required for STAT5-induced up-regulation of PIM-1 that favored cell proliferation and survival.

Deletion of the JM domain of FLT3 in EF1 retains the activations of PI3K and MAPK pathways

The above results showed that there was a linkage between IL-3-independent cell growth rate and the expression level of PIM-1 that seems not simply regulated by the activated STAT5 alone. Because expression of PIM-1 appears to reflect signaling by PI3K and MAPK pathways [24], we next analyzed phosphorylation status of these two pathways. We demonstrated here that expression of the EF1 fusion protein in Ba/F3 cells led to phosphorylation of both AKT and MAPK, in addition to STAT5 activation (Fig. 3C). These activations and up-regulation of PIM-1 as well as cell proliferation were further confirmed to be medicated through EF1 activity because they were all inhibited by a FLT3 specific inhibitor, PKC412 (Fig. 4). However, we also showed that there was not any direct linkage between activation of either AKT or MAPK and PIM-1 expression (Fig. 3B and C). The fact that deletion of the JM domain had no affect on the EF-mediated activations of STAT5, AKT, and MAPK but abrogated PIM-1 expression indicates that up-regulation of PIM-1 by EF1 might be independent of a requirement for signaling through these three pathways. How the mutated FLT3 up-regulates PIM-1 remains an area of active investigation.
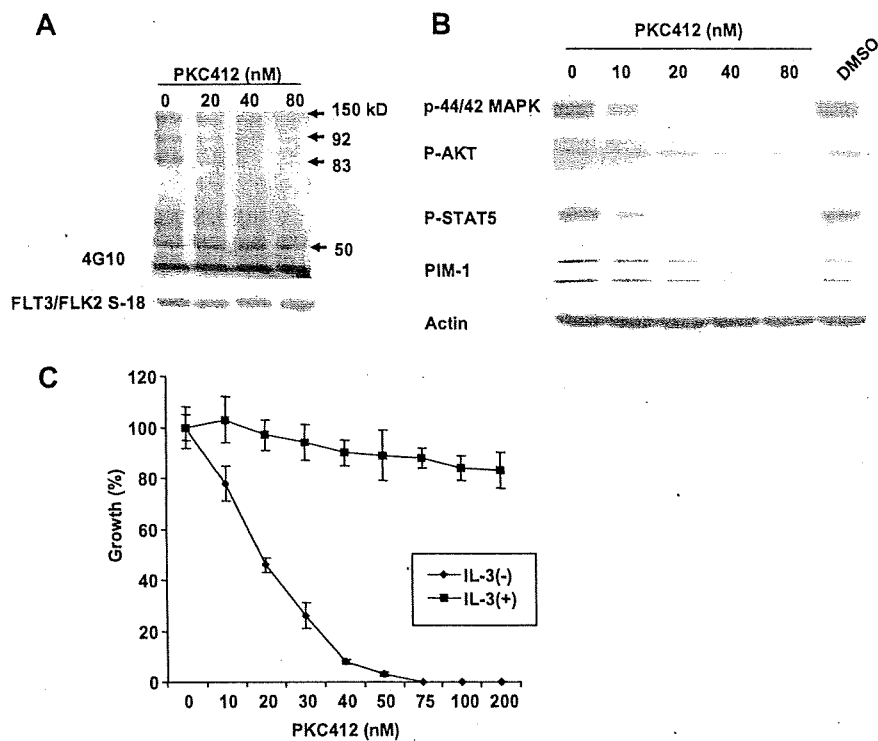
Fig. 4. Effects of PKC412 on Ba/F3-EF1 cells. (A) Inhibition of EF-mediated cellular tyrosine phosphorylation by PKC412. Ba/F3-EF1 cells were starved of IL-3 overnight and then treated with indicated concentrations of PKC412 for 4 h. Total cell lysates were immunoblotted with 4G10 (top panels) or FLT3/FLK2 S-18 (bottom panels). (B) Phosphorylations of STAT5, AKT and MAPK as well as expression of PIM-1 were inhibited by PKC412 in a dose-dependent manner. Total cell lysates were immunoblotted with specific antibodies. Cells cultured in medium with 0.1% DMSO was used as a control. (C) Inhibitory effect of PKC412 on the Ba/F3-EF1 cell growth. 5 × 10³ cells were seeded in each well of 96-well plates in the presence or absence of IL-3 with various concentrations of PKC412. After 72 h, TetraColor ONE cell proliferation assays were performed to measure the growth. Results are expressed as the percentage of the values measured when cells were grown in media without IL-3 and PKC412. The data presented are the average of three separate experiments.

References

[1] W. Matthews, C.T. Jordan, M. Gavin, N.A. Jenkins, N.G. Copeland, I.R. Lemischka, A receptor tyrosine kinase cDNA isolated from a population of enriched primitive hematopoietic cells and exhibiting close genetic linkage to c-kit, Proc. Natl. Acad. Sci. USA 88 (1991) 9026–9030.

[2] O. Rosnet, S. Marchetto, O. deLapeyriere, D. Birnbaum, Murine Flt3, a gene encoding a novel tyrosine kinase receptor of the PDGFR/CSF1R family, Oncogene 6 (1991) 1641–1650.

[3] O. Rosnet, C. Schiff, M.J. Pebusque, S. Marchetto, C. Tonnelle, Y. Toiron, F. Birg, D. Birnbaum, Human FLT3/FLK2 gene: cDNA cloning and expression in hematopoietic cells, Blood 82 (1993) 1110–1119.

[4] E. Heiss, K. Masson, C. Sundberg, M. Pedersen, J. Sun, S. Bengtsson, L. Ronnstrand, Identification of Y589 and Y599 in the juxtamembrane domain of Flt3 as ligand-induced autophosphorylation sites involved in binding of Src family kinases and the protein tyrosine phosphatase SHP2, Blood 108 (2006) 1542–1550.

[5] M.H. Tomasson, D.W. Sternberg, I.R. Williams, M. Carroll, D. Cain, J.C. Aster, R.L. Ilaria Jr., R.A. Van Etten, D.G. Gilliland, Fatal myeloproliferation, induced in mice by TEL/PDGFbetaR expression, depends on PDGFbetaR tyrosines 579/581, J. Clin. Invest. 105 (2000) 423–432.

[6] D.L. Stirewalt, J.P. Radich, The role of FLT3 in haematopoietic malignancies, Nat. Rev. Cancer 3 (2003) 650–665.

[7] M. Nakao, S. Yokota, T. Iwai, H. Kaneko, S. Horiike, K. Kashima, Y. Sonoda, T. Fujimoto, S. Misawa, Internal tandem duplication of the flt3 gene found in acute myeloid leukemia, Leukemia 10 (1996) 1911–1918.

[8] P.D. Kottaridis, R.E. Gale, M.E. Frew, G. Harrison, S.E. Langabeer, A.A. Belton, H. Walker, K. Wheatley, D.T. Bowen, A.K. Burnett, A.H. Goldstone, D.C. Linch, The presence of a FLT3 internal tandem duplication in patients with acute myeloid leukemia (AML) adds important prognostic information to cytogenetic risk group and response to the first cycle of chemotherapy: analysis of 854 patients from the United Kingdom Medical Research Council AML 10 and 12 trials, Blood 98 (2001) 1752–1759.

[9] S. Schnittger, C. Schoch, M. Dugas, W. Kern, P. Staib, C. Wuchter, H. Loffler, C.M. Sauerland, H. Serve, T. Buchner, T. Haferlach, W. Hiddemann, Analysis of FLT3 length mutations in 1003 patients with acute myeloid leukemia: correlation to cytogenetics, FAB subtype, and prognosis in the AMLCG study and usefulness as a marker for the detection of minimal residual disease, Blood 100 (2002) 59–66.

[10] C. Thiede, C. Steudel, B. Mohr, M. Schaich, U. Schakel, U. Platzbecker, M. Wermke, M. Bornhauser, M. Ritter, A. Neubauer, G. Ehninger, T. Illmer, Analysis of FLT3-activating mutations in 979 patients with acute myelogenous leukemia: association with FAB subtypes and identification of subgroups with poor prognosis, Blood 99 (2002) 4326–4335.

[11] C. Reindl, K. Bagrintseva, S. Vempati, S. Schnittger, J.W. Ellwart, K. Wenig, K.P. Hopfner, W. Hiddemann, K. Spiekermann, Point mutations in the juxtamembrane domain of FLT3 define a new class of activating mutations in AML, Blood 107 (2006) 3700–3707.

[12] C. Choudhary, J. Schwable, C. Brandts, L. Tickenbrock, B. Sargin, T. Kindler, T. Fischer, W.E. Berdel, C. Muller-Tidow, H. Serve, AML-associated Flt3 kinase domain mutations show signal transduction differences compared with Flt3 ITD mutations, Blood 106 (2005) 265–273.

[13] J.L. Rocnik, R. Okabe, J.C. Yu, B.H. Lee, N. Giese, D.P. Schenkein, D.G. Gilliland, Roles of tyrosine 589 and 591 in STAT5 activation and transformation mediated by FLT3-ITD, Blood 108 (2006) 1339–1345.

[14] K. Bagrintseva, S. Geisenhof, R. Kern, S. Eichenlaub, C. Reindl, J.W. Ellwart, W. Hiddemann, K. Spiekermann, FLT3-ITD-TKD dual mutants associated with AML confer resistance to FLT3 PTK inhibitors and cytotoxic agents by overexpression of Bcl-x(L), Blood 105 (2005) 3679–3685.

[15] R. Grundler, C. Thiede, C. Miething, C. Steudel, C. Peschel, J. Duyster, Sensitivity toward tyrosine kinase inhibitors varies between different activating mutations of the FLT3 receptor, Blood 102 (2003) 646–651.

[16] C. Choudhary, C. Muller-Tidow, W.E. Berdel, H. Serve, Signal transduction of oncogenic Flt3, Int. J. Hematol. 82 (2005) 93–99.

[17] H.A. Vu, P.T. Xinh, M. Masuda, T. Motoji, A. Toyoda, Y. Sakaki, K. Tokunaga, Y. Sato, FLT3 is fused to ETV6 in a myeloproliferative disorder with hypereosinophilia and a t(12;13)(p13;q12) translocation, Leukemia 20 (2006) 1414–1421.

[18] M. Benekli, M.R. Baer, H. Baumann, M. Wetzler, Signal transducer and activator of transcription proteins in leukemias, Blood 101 (2003) 2940–2954.

[19] K. Murata, H. Kumagai, T. Kawashima, K. Tamitsu, M. Irie, H. Nakajima, S. Suzu, M. Shibuya, S. Kamihira, T. Nosaka, S. Asano, T. Kitamura, Selective cytotoxic mechanism of GTP-14564, a novel tyrosine kinase inhibitor in leukemia cells expressing a constitutively active Fms-like tyrosine kinase 3 (FLT3), J. Biol. Chem. 278 (2003) 32892–32898.

[20] H. Kiyoi, R. Ohno, R. Ueda, H. Saito, T. Naoe, Mechanism of constitutive activation of FLT3 with internal tandem duplication in the juxtamembrane domain, Oncogene 21 (2002) 2555–2563.

[21] K.T. Kim, K. Baird, J.Y. Ahn, P. Meltzer, M. Lilly, M. Levis, D. Small, Pim-1 is up-regulated by constitutively activated FLT3 and plays a role in FLT3-mediated cell survival, Blood 105 (2005) 1759–1767.

[22] K.T. Kim, M. Levis, D. Small, Constitutively activated FLT3 phosphorylates BAD partially through Pim-1, Br. J. Haematol. 134 (2009) 500–509.

[23] G. Wernig, J.R. Gonneville, B.J. Crowley, M.S. Rodrigues, M.M. Reddy, H.E. Hudon, C. Walz, A. Reiter, K. Podar, Y. Royer, S.N. Constantinescu, M.H. Tomasson, J.D. Griffin, D.G. Gilliland, M. Sattler, The Jak2V617F oncogene associated with myeloproliferative diseases requires a functional FERM domain for transformation and for expression of the Myc and Pim proto-oncogenes, Blood 111 (2008) 3751–3759.

[24] J.S. Krumenacker, V.S. Narang, D.J. Buckley, A.R. Buckley, Prolactin signaling to pim-1 expression: a role for phosphatidylinositol 3-kinase, J. Neuroimmunol. 113 (2001) 249–259.

ORIGINAL ARTICLE

A phase II trial of weekly chemotherapy with paclitaxel plus gemcitabine as a first-line treatment in advanced non-small-cell lung cancer

Kiyoshi Mori · Hiroyuki Kobayashi ·
Yukari Kamiyama · Yasuhiko Kano · Tetsuro Kodama

Abstract

Purpose The efficacy and toxicity of combined paclitaxel (PTX) and gemcitabine (GEM) was evaluated as a protocol for first-line chemotherapy in 40 patients with advanced non-small-cell lung cancer (NSCLC).

Methods Paclitaxel, 100 mg/m², was administered intravenously (IV) as a 1-h infusion, followed by GEM, 1,000 mg/m², IV over 30 min on days 1 and 8 of a 21-day cycle. The median age of patients was 66 years with a range of 33–75 years. Nearly all patients (39/40) had an ECOG performance status of 0 or 1. Thirteen patients (32%) had initial stage IIIB disease and 27 patients (68%) had stage IV disease. Histological subtypes were adenocarcinoma (73%) and squamous cell carcinoma (25%).

Results Twenty-two patients (55%) achieved a partial response and none achieved a complete response, giving an overall response rate of 55% (95% confidence interval: 38.2–71.8%). Disease stability was achieved in 14 patients (35%), and 4 patients (10%) had progressive disease. The median survival time was 11.9 months (95% CI: 10.3–14 months), with a 1-year survival rate of 47.5%. Grade 3 or 4 hematological toxicities observed included neutropenia in 37.5%, anemia in 2.5%, and thrombocytopenia in 5.0% of these patients. Non-hematologic toxicities were mild, with the exception of grade 3 and 4 pneumonitis. There were no deaths due to toxicity.

Conclusion Weekly chemotherapy with PTX plus GEM is effective and is acceptable for the first line treatment of advanced NSCLC.

Keywords Non-small-cell lung cancer · First-line chemotherapy · Weekly chemotherapy · Gemcitabine · Paclitaxel

K. Mori (✉) · H. Kobayashi · Y. Kamiyama · Y. Kano · T. Kodama
Division of Thoracic Oncology,
Department of Medical Oncology, Tochigi Cancer Center,
4-9-13, Yohnan, Utsunomiya, Tochigi 320-0834, Japan
e-mail: kmori@tcc.pref.tochigi.jp

H. Kobayashi
e-mail: kobahiro@jichi.ac.jp

Y. Kamiyama
e-mail: ykamiyam@tcc.pref.tochigi.jp

Y. Kano
e-mail: ykano@tcc.pref.tochigi.jp

T. Kodama
e-mail: tkodama@tcc.pref.tochigi.jp

Introduction

Lung cancer ranks among the most commonly occurring malignancies and currently is the leading cause of cancer-related deaths worldwide [21]. In Japan lung cancer is responsible for approximately 55,000 cancer-related deaths per year [5]. Even though the clinical usefulness of first-line chemotherapy has been established for the cases of advanced non-small-cell lung cancer (NSCLC), the prognosis is still extremely poor.

A number of new agents have become available recently for the treatment of unresectable and metastatic NSCLC in Japan, including the taxanes, gemcitabine (GEM), and vinorelbine. In randomized phase III trials, these agents in combination with a platinum compound have been associated with improved survival of patients having advanced NSCLC [8, 17, 23, 24]. However, a platinum compound is associated with a greater toxicity than other drugs used to treat NSCLC. In addition to nausea and vomiting, it causes neuropathy, profound fatigue, and renal toxicity. Some

patients are unable to tolerate the drug toxicity and terminate treatment early. Based on these observations, non-platinum regimens have been proposed as an alternative to the platinum-based combinations for treatment of advanced NSCLC [13].

Paclitaxel (PTX) and GEM are new anti-cancer agents having significant single-agent activity against advanced NSCLC. A recent clinical phase II study of 122 patients with previously untreated, unresectable stage III or IV NSCLC receiving a 3-h infusion of PTX at a dose of 210 mg/m^2 showed a good response rate of 35% [25]. Although PTX is usually given once every 3 weeks, Chan et al. [10] demonstrated that weekly administration of PTX at a dose of 80–90 mg/m^2 provides similar tolerability and a possible increase in efficacy.

Gemcitabine, a novel deoxycytidine analog, had a response rate of 20% with a single weekly administration in previously untreated advanced NSCLC [4]. As a first-line treatment, single-agent GEM has been shown to have anti-tumor activity equal to that of cisplatin/etoposide, resulting in less toxicity and a slightly better quality of life [27].

These agents have different mechanisms of action, and their toxicities are partially non-overlapping. Although the usual administration of PTX is once every 3 weeks, a weekly administration can increase efficacy with good tolerability [1, 2]. We demonstrated that weekly administration with PTX and GEM is a tolerable and active regimen for patients with advanced NSCLC previously treated with platinum-containing chemotherapy regimens [20]. Based on these findings, we designed a phase II trial to examine the efficacy and tolerance of the non-platinum-based combination of PTX and GEM administered weekly for patients with untreated advanced NSCLC.

Patients and methods

Patient selection

All patients with histologically or cytologically confirmed advanced NSCLC were eligible for this phase II trial. The subjects of this study were patients with clinical stage IV NSCLC or stage III with unresectable disease or for whom radiotherapy with curative intent is not possible. Patients with unresectable disease or radiotherapy with curative intent is not possible include those with pleural effusion and dissemination, those with intrapulmonary metastasis within the ipsilateral lobe, those with an irradiation field exceeding one-half of one lung, those with metastasis to the contralateral hilar lymph nodes, and those with reduced lung function. Other eligibility criteria included: age older than 20 years and younger than 76 years; Eastern Cooperative

Oncology Group (ECOG) performance status (PS) of 0–2; measurable lesions; life expectancy ≥ 12 weeks; adequate bone marrow reserve with a WBC count $\geq 4,000$ per mm^3; platelet count $\geq 10 \times 10^4$ per mm^3; and hemoglobin level ≥ 9.0 g/dL; liver function with a AST and ALT $\leq 2.5 \times$ upper normal limit, unless as a result of liver metastases; and adequate renal function with a serum creatinine level ≤ 1.5 mg/dL. No prior radiotherapy treatment was allowed if the irradiated area was not the site of measurable lesion and the therapy was completed at least 2 weeks before enrollment into the study.

Patients were excluded for the following indications: ≥ 76 years of age (vinorelbine as single agent treatment), severe cardiovascular or cerebrovascular disease, uncontrolled diabetes or hypertension, active infection, pulmonary fibrosis, massive pleural effusion or ascites, active peptic ulcer, and severe neurological disorders. Patients were also excluded in case of previous malignancy and any evidence or history of hypersensitivity or other contraindications for the drugs used in this trial. Written informed consent was obtained from all patients.

Treatment

Paclitaxel, 100 mg/m^2, was administered IV during a 1-h infusion, followed by GEM, 1,000 mg/m^2, IV over 30 min on days 1 and 8 of 21-day cycle. Premedication for PTX consisted of dexamethasone 20 mg, diphenhydramine 50 mg, and ranitidine 50 mg IV for 30 min before PTX infusion. After the premedication for PTX was completed, a serotonin receptor antagonist was given as a 30-min infusion for prophylactic antiemetic therapy. Treatment was repeated every 3 weeks until maximum response plus two cycles or unacceptable toxicity. In stable disease, patients received a maximum of six cycles. At the investigator's discretion, patients were treated with up to eight cycles of the drug combination.

Dose modifications were planned according to hematologic and severe non-hematologic toxic effects. Once the doses were reduced, they were not increased. Patients who experienced grade 4 neutropenia, grade 4 thrombocytopenia, reversible grade 2 neurotoxicity, or liver dysfunction received reduced doses of both PTX, 75 mg/m^2, and GEM, 800 mg/m^2, for the next cycle. The next course of chemotherapy was started after 3 weeks when the leukocyte count was 3,000 per mm^3 or greater, the neutrophil count was 1,500 per mm^3 or greater, the platelet count was 75,000 per mm^3 or greater, serum creatinine was less than 1.5 mg/dL, GOT and GPT were less than twice the upper limit of the normal range, and the neurotoxicity was grade 1 or less. If hematologic recovery was not achieved by day 35 of treatment, the patient was withdrawn from the study.

Evaluation of responses and toxicity

Responses and toxicity were evaluated on the basis of tumor images obtained by computerized tomography (CT), laboratory results, subjective/objective symptoms, signs before, during, and after administration of the study drugs and during the period from completion of treatment to the final analysis. Measurable disease parameters were determined every 4 weeks by various means such as CT. Evaluation was performed in compliance with the response evaluation criteria in solid tumors (RECIST) guidelines for anti-tumor activity. Adverse events were assessed using the Common Terminology Criteria for Adverse Events version 3.0 (CTCAEv3.0). Patients were withdrawn from the study if evidence of tumor progression was observed. The institutional ethical review committee gave approval to the study.

Statistical analysis

The primary end point of the study was the response rate. Simon's two-stage design was used to determine sample size and decision criteria. It was assumed that a response rate of 40% in eligible patients would indicate potential usefulness, while a rate of 20% would be the lower limit of interest; $\alpha = 0.05$ and $\beta = 0.10$. Using these design parameters, the first stage of the study was to enroll 24 patients, and the regimen was rejected if fewer than five patients had an objective response. If six or more patients responded, the accrual was continued until 45 patients were enrolled (45 patients were required because of anticipated percentage of dropout cases). Combination therapy was considered effective if ≥ 14 of the 45 patients showed a response in the final analysis. Secondary end points were toxicity and overall survival. Response and survival rates were both calculated on an intent-to-treat basis. Overall survival and time to progression were measured from the start of this treatment until time of death or the date of the last follow-up clinical assessment. Survival curves were constructed using the Kaplan–Meier method (Fig. 1).

Results

Patient characteristics

A total of 40 patients were enrolled in the study between September 2001 and July 2004. The majority of patients were treated as outpatients. The clinical characteristics of the patients are listed in Table 1. The median age was 66 years with a range of 33–75 years. Nearly two-thirds of the patients were men. Twenty-four patients had an PS
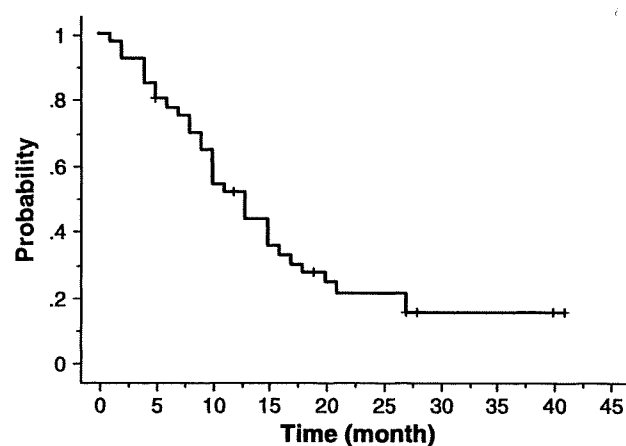

Fig. 1 Kaplan–Meier estimated overall survival curves. Median survival time, 11.9 months; 1-year survival rate, 47.5%

Table 1 Patient characteristics

Eligible patients	40
Gender	
Male	26
Female	14
Age (years)	
Median	66
Range	33–75
Performance status	
0	24
1	15
2	1
Histology	
Adenocarcinoma	29
Squamous cell	10
Large cell	1
Stage	
III	13
IV	27
Number of metastatic sites	
Median	2
Range	0–3
Location of metastases	
Bone	12
Lung nodules	10
Liver	9
Lymph nodes	8
Adrenals	6
Brain	3
Subcutaneous	1

of 0, and 15 had PS of 1. Histological subtypes were 73% (29/40) adenocarcinoma and 25% (10/40) squamous cell carcinoma.

Toxicities

The toxicities observed during this study are provided in Table 2. Hematological toxicities were the most common, but grade 3–4 toxicities, including neutropenia (37.5%), thrombocytopenia (5.0%), and anemia (2.5%) were relatively modest. There were only two cases of febrile neutropenia (5.0%). Grade 1 nausea, fatigue, alopecia, neuropathy, and angialgia occurred with a greater frequency than the non-hematologic toxicities. Grade 3–4 non-hematologic toxicities were not seen except in cases of pulmonary toxicity. Two patients (5.0%) developed interstitial pneumonitis (grade 3; one patient, grade 4; one patient), and were responsive to steroid therapy.

Efficacy of treatment

The median number of cycles administered per patient was 4, and the number of cycles ranged from 1 to 8. Twenty-two patients exhibited a partial response. The overall response rate was 55% (22/40) [95% confidence interval (CI): 38.2–71.8%]. Stable disease was achieved in 14 patients (35%), and 4 patients (10%) had progressive disease. All 40 patients were included in the survival analysis. The overall median survival time was 11.9 months (95% CI: 10.3–14 months). The 1-year survival rate was 47.5% (19/40). The median time to disease progression was 6.4 months. Thirty patients (75%) received chemotherapy, and 4 patients (10%) received thoracic irradiation as second-line treatment.

Discussion

Although a standard regimen of first-line chemotherapy for advanced NSCLC is being established, it is important to develop a more active and well-tolerated regimen. Several published randomized studies reported that non-platinum-

Table 2 Maximum toxicity over 40 patients

	CTCAE v 3.0 grade (no. of patients)		Grade 3 or 4 (%)
	Grade 3	Grade 4	
Leukopenia	11	1	12 (30)
Neutropenia	11	4	15 (37.5)
Febrile neutropenia	2	0	2 (5.0)
Anemia	1	0	1 (2.5)
Thrombocytopenia	2	0	2 (5.0)
Pneumonitis	1	1	2 (5.0)

CTCAE v 3.0: Common Terminology Criteria for Adverse Events version 3.0

based chemotherapy in advanced NSCLC was as effective and less toxic than platinum-based regimens [13, 15, 18, 29]. Georgoulias et al. [13] compared the combination of a cisplatin and docetaxel regimen with the GEM and docetaxel regimen. Objective response rates were similar in the two groups, with 32.4% in the former and 30.2% in the latter. The two groups did not differ in the overall survival or 1- or 2-year survival rates. They concluded that both drug combinations had comparable activity and the non-platinum-based regimen had the more favorable profile.

Generally, non-cisplatin-containing treatment does not require supplemental hydration as does standard cisplatin-based chemotherapy. This may be advantageous for elderly patients, patients with poor PS, and patients with renal or cardiac impairment. Recchia et al. [22] conducted a trial of PTX plus GEM in advanced NSCLC patients with a low PS. The chemotherapy regimen consisted of 200 mg/m^2 PTX on day 1 plus 1,000 mg/m^2 GEM on days 1 and 8, repeated every 3 weeks, for a maximum of eight cycles. They achieved a reasonable response rate of 41.3%. Median overall survival time was 13.6 months; the authors concluded that a satisfactory clinical benefit could be obtained with GEM plus PTX regimen in NSCLC patients with a poor PS.

Thus, non-platinum-based chemotherapy may be used as alternative to platinum-based regimens. We conducted a phase II trial was designed to examine the efficacy and tolerance of the non-platinum-based combination of weekly PTX and GEM for patients with untreated advanced NSCLC. Results including an overall response rate of 55%, a median survival time of 11.9 months, and a 1-year survival probability rate of 47.5% suggested that this regimen might have anti-tumor activity equal to that of platinum-based regimens.

Weekly chemotherapy for lung cancer has recently been carried out at several facilities, and favorable results were reported [9, 16, 26, 30]. Compared to standard chemotherapy with administration of drugs at intervals of 3–4 weeks, weekly chemotherapy appears acceptable for the reduction of a single dose level of anti-cancer drugs with fewer side effects. In addition, weekly dose level is more easily adjusted according to the general clinical condition of individual patients or if hematologic toxicity develops. Belani et al. [6] conducted a randomized phase II trial of a 3-week schedule of GEM plus PTX (ArmA) versus a weekly schedule of GEM plus PTX (ArmB) in the treatment of NSCLC. It was concluded that a weekly schedule resulted in improved survival and lower hematologic toxicity than the 3-week schedule.

The clinical outcomes of weekly PTX and GEM therapy found in the literature [3, 6, 7, 11, 12, 14, 19, 28] and in our results are summarized in Table 3. The response rate ranges were from 23.1 to 55%; overall median survival time was 4.9–11.9 months; and 1-year survival rates were 26–53%. Most adverse reactions were hematologic (such as leukope-

Table 3 PG regimens used as first-line treatment of advanced NSCLC

First author (ref.)	No. of patients		Regimen and schedule	Response rate (%)	Survival median	One-year (%)
Belani et al. [6]	50	Arm A	P 200 mg/m² day 1 q3w	28.2	7.5	34
			G 1 g/m² days 1, 8 q3w			
	50	Arm B	P 100 mg/m² days 1, 8 q 3w	26.8	9.6	42
			G 1 g/m² days 1, 8 q3w			
Bhatia et al. [7]	39		P 110 mg/m² days 1, 8, 15 q 4w	38.2	4.9	26
			G 1 g/m² days 1, 8, 15 q4w			
De Pas et al. [12]	54		P 100 mg/m² days 1, 8, 15, 22 q 4w	46	9.6	53
			G 1 g/m² days 1, 8, 15, 22 q4w			
Akerley et al. [3]	39		P 85 mg/m² days 1, 8, 15, 22, 29, 36 q 8w	23.1	7.5	32
			G 1 g/m² days 1, 8, 15, 22, 29, 36 q8w			
Gillenwater et al. [14]	39		P 100 mg/m² days 1, 8, 15, 21 q 4w	35	4.9	35
			G 1 g/m² days 1, 8, 15, 21 q4w			
Kosmidis et al. [19]	225		P 200 mg/m² day 1 q 3w	31	9.3	42
			G 1 g/m² days 1, 8, q3w			
Treat et al. [28]	312		P 200 mg/m² day 1 q 3w	43.6	8.4	33
			G 1 g/m² days 1, 8, q3w			
Our study	40		P 100 mg/m² days 1, 8, q 3w	55	11.9	47.5
			G 1 g/m² days 1, 8 q3w			

NSCLC non-small-cell lung cancer, *P* paclitaxel, *G* demcitabine

nia and neutropenia of grade 3 or greater occurrence) in 28–53%. Variable toxicities may be due to population-related pharmacogenomics [11]. Overall, the non-hematologic toxicity was mild, and there were few adverse reactions of grade 3 or greater. A few patients had pneumonitis which was not responsive to steroid therapy. The treatment in our current study was reasonably tolerated, especially in the area of non-hematologic toxicity. Nausea, vomiting, and fatigue, which are often seen in cisplatin-containing regimens, were relatively mild; no patients developed renal toxicity.

In conclusion, weekly chemotherapy with PTX and GEM is a well-tolerated and effective regimen for previously untreated patients with advanced NSCLC. Further studies are expected for the application of this regimen to the elderly, and patients with a poor PS or suspected vulnerability to platinum compound toxicity.

Conflict of interest statement None.

References

1. Akerley W 3rd (2000) Paclitaxel in advanced non-small cell lung cancer: an alternative high-dose weekly schedule. Chest 117(4 Suppl 1):152S–155S

2. Akerley W, Rathore R, Ready N, Leone L, Sikov W, Safran H et al (2002) A phase I study of a weekly schedule of paclitaxel and carboplatin in patients with advanced carcinoma. Cancer 95:2000–2005
3. Akerley W, Safran H, Zaner K, Ready N, Mega T, Kennedy T (2006) Phase II trial of weekly paclitaxel and gemcitabine for previously untreated, stage IIIB-IV nonsmall cell lung cancer. Cancer 107:1050–1054
4. Anderson H, Lund B, Bach F, Thatcher N, Walling J, Hansen HH (1994) Single-agent activity of weekly gemcitabine in advanced non-small cell lung cancer: a phase II study. J Clin Oncol 12:1821–1826
5. Ando M, Wakai K, Seki N, Tamakoshi A, Suzuki K, Ito Y et al (2003) Attributable and absolute risk of lung cancer death by smoking status: findings from the Japan collaborative cohort study. Int J Cancer 105:249–254
6. Belani CP, Dakhil S, Waterhouse DM, Desch CE, Rooney DK, Clark RH et al (2007) Randomized phase II trial of gemcitabine plus weekly versus three-weekly paclitaxel in previously untreated advanced non-small cell lung cancer. Ann Oncol 18:110–115
7. Bhatia S, Hanna N, Ansari R, Pletcher W, Einhorn L, Sandler A et al (2002) A Phase II study of weekly gemcitabine and paclitaxel in patients with previously untreated stage IIIb and IV non-small cell lung cancer. Lung Cancer 38:73–77
8. Bonomi P, Kim K, Kusler J, Johnson D (1997) Cisplatin/etoposide vs paclitaxel/cisplatin/G-CSF vs paclitaxel/cisplatin in non-small-cell lung cancer. Oncology (Williston Park) 4(Suppl 3):9–10
9. Buccheri G, Ferrigno D (2004) Cuneo lung cancer study group. Second-line weekly paclitaxel in patients with inoperable non-small cell lung cancer who fail combination chemotherapy with cisplatin. Lung Cancer 45:227–236
10. Chang AY, Rubins J, Asbury R, Boros L, Hui LF (2001) Weekly paclitaxel in advanced non-small cell lung cancer. Semin Oncol 28(4 Suppl 14):10–13
11. Crowley J, Furuse K, Kawahara M, Fukushima M, Kawaguchi T, Williamson S et al (2006) Second Japan-SWOG common arm

analysis of paclitaxel/carboplatin in advanced stage non-small cell lung cancer (NSCLC): a model for testing population-related pharmacogenomics (#7050). Proc Am Soc Clin Oncol 24:376S

12. De Pas T, Putzu C, Curigliano G, Noberasco C, Sabrina B, Catania C et al (2006) A proper schedule of weekly paclitaxel and gemcitabine combination is highly active and very well tolerated in NSCLC patients. Lung Cancer 54:359–364

13. Georgoulias V, Papadakis E, Alexopoulos A, Tsiafaki X, Rapti A, Veslemes M et al (2001) Platinum-based and non-platinum-based chemotherapy in advanced non-small-cell lung cancer: a randomized multicentre trial. Lancet 357:1478–1484

14. Gillenwater HH, Stinchcombe TE, Qaqish BF, Tyann M, Hensing TA, Socinski MA (2005) A phase II trial of weekly paclitaxel and gemctiabine infused at a constant rate in patients with advanced non-small cell lung cancer. Lung Cancer 47:413–419

15. Gridelli C, Perrone F, Palmeri S, D'Aprile M, Cognetti F, Rossi A et al (1996) Mitomycin C plus vindesine plus etoposide(MEV) versus mitomycin C plus vindesine plus cisplatin(MVP) in stage IV non-small-cell lung cancer: A phase III multicentre randomised trial. The "Gruppo Oncologico Centro-Sud-Isole" (G.O.C.S.I.). Ann Oncol 7:821–826

16. Juan O, Albert A, Ordono F, Casany R, Caranana V, Campos JM et al (2002) Low-dose weekly paclitaxel as second-line treatment for advanced non-small cell lung cancer: a phase II study. Jpn J Clin Oncol 32:449–454

17. Kelly K, Crowley J, Bunn PA Jr, Presant CA, Grevstad PK, Moinpour CM et al (2001) Randomized phase III trial of paclitaxel plus carboplatin versus vinorelbine plus cisplatin in the treatment of patients with advanced non-small-cell lung cancer: a southwest oncology group trial. J Clin Oncol 19:3210–3218

18. Kosmidis P, Mylonakis N, Nicolaides C, Kalophonos C, Samantas E, Boukovinas J et al (2002) Paclitaxel plus carboplatin versus gemcitabine plus paclitaxel in advanced non-small-cell lung cancer: a phase III randomized trial. J Clin Oncol 20:3578–3585

19. Kosmidis PA, Kalofonos HP, Christodoulou C, Syrigos K, Makatsoris T, Skarlos D et al (2008) Paclitaxel and gemcitabine versus carboplatin and gemcitabine in patients with advanced non-small-cell lung cancer. A phase III study of the Hellenic cooperative oncology group. Ann Oncol 19:115–122

20. Mori K, Kamiyama Y, Kondo T, Kano Y, Kodama T (2007) Phase II study of weekly chemotherapy with paclitaxel and gemcitabine as second-line treatment for advanced non-small cell lung cancer

after treatment with platinum-based chemotherapy. Cancer Chemother Pharmacol 60:189–195

21. Peto R, Chen ZM, Boreham J (1999) Tobacco—the growing epidemic. Nat Med 5:15–17

22. Recchia F, Saggio G, Cesta A, Candeloro G, Rea S (2005) Paclitaxel plus gemcitabine in advanced non-small cell lung cancer patients with low performance status. Anticancer Res 25:409–414

23. Scagliotti GV, De Marinis F, Rinaldi M, Crino L, Gridelli C, Ricci S et al (2002) Italian lung cancer project. Phase III randomized trial comparing three platinum-based doublets in advanced non-small-cell lung cancer. J Clin Oncol 20:4285–4291

24. Schiller JH, Harrington D, Belani CP, Langer C, Sander A, Krook J et al (2002) Comparison of four chemotherapy regimens for advanced non-small-cell lung cancer. N Engl J Med 346:92–98

25. Sekine I, Nishiwaki Y, Watanabe K, Yoneda S, Saijo N (1996) Phase II study of 3-hour infusion of paclitaxel in previously untreated non-small cell lung cancer. Clin Cancer Res 2:941–945

26. Socinski MA, Schell MJ, Bakri K, Peterman A, Lee JH, Unger P et al (2002) Second-line, low-dose, weekly paclitaxel in patients with stage IIIB/IV nonsmall cell lung carcinoma who fail first-line chemotherapy with carboplatin plus paclitaxel. Cancer 95:1265–1273

27. ten Bokkel Huinink WW, Bergman B, Chemaissani A, Dornoff W, Drings P, Kellokumpu-Lehtinen PL et al (1999) Single-agent gemcitabine: an active and better tolerated alternative to standard cisplatin-based chemotherapy in locally advanced or metastatic non-small cell lung cancer. Lung Cancer 26:85–94

28. Treat J, Belani CP, Edelman MJ, Socinski MA, Ansari RH, Obasaju CK et al (2005) A randomized phase III trial of gemcitabine (G) in combination with carboplatin (C) or paclitaxel (P) versus paclitaxel plus carboplatin in advanced (Stage IIIB, IV) non-small cell lung cancer (NSCLC): updata of the Alpha Oncology trial (A1-99002L). (#7025). Proc Am Soc Clin Oncol 23:1096S

29. Yamamoto N, Fukuoka M, Negoro SI, Nakagawa K, Saito H, Matsui K et al (2004) Randomised phase II study of docetaxel/cisplatin vs docetaxel/irinotecan in advanced non-small-cell lung cancer: a West Japan thoracic oncology group study (WJTOG9803). Br J Cancer 90:87–92

30. Yasuda K, Igishi T, Kawasaki Y, Kato K, Matsumoto S, Katayama S et al (2004) Phase II study of weekly paclitaxel in patients with non-small cell lung cancer who have failed previous treatments. Oncology 66:347–352